JOURNAL OF SOLID STATE CHEMISTRY 91, 16–24 (1991)

Synthesis and Properties of Nitrite–Nitrate Sodalite Solid Solutions $Na_8[AlSiO_4]_6(NO_2)_{2-x}(NO_3)_x$; $0.4 \leq x \leq 1.8$

JOSEF CHRISTIAN BUHL

Institut für Mineralogie, Universität Münster, Corrensstr. 24, D-4400 Münster, Federal Republic of Germany

Received July 9, 1990; in revised form September 24, 1990

Nitrite–nitrate sodalite $Na_8[AlSiO_4]_6(NO_2)_{2-x}(NO_3)_x$ ($0.4 \leq x \leq 1.8$) solid solutions have been prepared using different methods: by hydrothermal synthesis in the presence of $NaNO_3$ at temperatures between 770 and 970 K ("direct" preparation) and by high-temperature oxidation of previously synthesized nitrite sodalite in air ("indirect" preparation). Both methods yield sodalites, imbibing a maximal amount of 90% nitrate within their cages. The oxidation process is characterized by the continuous weight uptake of the crystals during heating as well as by a rising unit cell volume according X-ray powder diffraction studies. A temperature of 1050 K could be estimated as the favorable value for this reaction inside the sodalite cages. The properties of the members of the new solid solution series have been studied by simultaneous thermal analysis, high-temperature X-ray diffraction, and IR spectroscopy. A reversible expansion of the unit cell volume at temperatures >920 K indicates orientational disorder and a high degree of intracage dynamics of the nitrite and nitrate guest species.

Introduction

Sodalites can be synthesized with a large variety of guest molecules located in the polyhedral cavities (*1–4*). Inclusion of several guest species yields new information on the reactivity and thermal stability of porous tectosilicates (*5,6*). In this connection sodalites are also an attractive model system for the zeolites A and X;Y, consisting of sodalite cages as basic structural building blocks (*7*).

Because recent investigations on the hydrothermal synthesis of sodium nitrite-imbibed sodalites gave evidence for a partial transformation of NO_2^- to NO_3^- within their polyhedral cages (*8,9*), some aspects of the high-temperature synthesis of nitrite–nitrate intercalated sodalites are investigated here. In addition to the study of hydrothermal synthesis this paper reports on the characterization of the observed products by X-ray powder diffraction, IR spectroscopy, and thermoanalytical methods.

Furthermore, a study of another preparation method for nitrite–nitrate sodalites based on a high-temperature oxidation in air, recently observed by different authors (*10–12*), is given. The products of this "indirect" way of formation of nitrate inside the sodalite cages are compared with the direct hydrothermally grown species and characterized by X-ray powder diffraction, IR spectroscopy, and simultaneous thermal analysis.

Experimental

Single crystals of sodium nitrite- and sodium nitrate-filled sodalites have been syn-

0022-4596/91 $3.00

TABLE I

THE CONDITIONS AND RESULTS OF THE HYDROTHERMAL SYNTHESES

No.	Starting material	Temperature (K)	Pressure (GPa)	Products	Cell parameter (Å)
1	Kaolinite	470	0.02	SOD[a]; $n = 0.25$	8.931(1)
2	Kaolinite (sintered)	770	0.15	SOD[b] $x = 0.4$	8.953(1)
3	Kaolinite (sintered)	870	0.15	SOD; $x = 1.0$	8.962(2)
4	Kaolinite (sintered)	970	0.20	SOD; $x = 1.8$	8.989(1)

[a] SOD, Sodalite $Na_8[AlSiO_4]_6(NO_2)_{2-n}(OH \cdot H_2O)_n$.
[b] SOD, Sodalite $Na_8[AlSiO_4]_6(NO_2)_{2-x}(NO_3)_x$.

thesized hydrothermally at temperatures of 770–970 K and pressures of 0.15–0.20 GPa in 18-ml steel autoclaves. Sealed silver tubes of 8 mm diameter and 100 mm length have been used as sample liners. The starting substances were prepared by heating kaolin (Fluka 60609) for 2 hr at 1700 K. This material (50 mg) was mixed with 270 mg of $NaNO_2$ (Riedel-deHaen 31443) and sealed together with 1 ml of an 8 *M* NaOH solution (Merck 836) into the silver tubes. After a reaction period of 2 days the products were washed with H_2O and prepared for X-ray Guinier powder analysis ($CuK\alpha_1$ radiation, 40 kV at 30 mA) and IR spectroscopy, using a Perkin–Elmer 683 spectrometer (KBr-pellets). Additional X-ray heating experiments (Enraf-Nonius Guinier-Simon camera) and simultaneous thermal analysis (Mettler 146 thermoanalyzer) have been carried out to study the thermal decomposition behavior of the new sodalite solid solutions. Common nitrite sodalite, first obtained by Hund (*2*) and synthesized in 50-ml Teflon-coated steel autoclaves as described in (*10,13*), has been taken as the "reference" for the evaluation of nitrate at elevated temperatures and pressures.

Polycrystalline powder of pure nitrite sodalite $Na_8[AlSiO_4]_6(NO_2)_{2-n}(OH \cdot H_2O)_n$ ($n = 0.2$) (reference material) and single crystals from experiment No. 6 of Table III have been used as initial material for the high-temperature oxidation studies. Three temperatures (800, 1050, and 1100 K) and different air flow rates (10 and 20 liters/hr) have been employed. The Mettler thermoanalyzer 146 has been used for the heating experiments to characterize the uptake of oxygen by thermogravimetry and differential thermal analysis. Sodalite powder (100 mg) was used in every run (Pt-crucibles; heating rates 8 and 25 K/min). After heating, the products were investigated by Guinier X-ray powder diffraction, IR spectroscopy, and simultaneous thermal analysis, as described above for the species obtained from "direct" hydrothermal syntheses.

Results and Discussion

Hydrothermal Synthesis (Direct Preparation Method)

The experimental parameters and the resulting phases are summarized in Table I. Nitrite–nitrate sodalites could be obtained exclusively in the whole temperature interval between 770 and 970 K, i.e., the crystallization of solid solutions in the composition range of $Na_8[AlSiO_4]_6(NO_2)_{2-x}(NO_3)_x$ ($0.4 \leq x \leq 1.8$) occurs, indicated by a rise of the unit cell parameter a_0 due to an increase of the nitrate content. (For values x and a_0 see Table I.) This nitrate content is the result of an oxidation process of the nitrite in the hydrothermal environment at high tempera-

TABLE II

X-RAY POWDER DATA OF NITRITE (NITRATE) SODALITE AND NITRATE (NITRITE) SODALITE, OBTAINED FROM HYDROTHERMAL SYNTHESIS

$Na_8[AlSiO_4]_6(NO_2)_{1.6}(NO_3)_{0.4}$ No. 2, Table I, cubic, a_0 = 8.953(1) Å				$Na_8[AlSiO_4]_6(NO_2)_{0.2}(NO_3)_{1.8}$ No. 4, Table I, cubic, a_0 = 8.989(1) Å			
h k l	$2\theta_{obs}$	d_{obs}	I/I_0	*h k l*	$2\theta_{obs}$	d_{obs}	I/I_0
1 1 0	13.981	6.329	66	1 1 0	13.949	6.344	60
2 0 0	19.831	4.473	17	2 0 0	19.763	4.489	22
2 1 0	22.157	4.010	3	2 1 0	22.117	4.016	6
2 1 1	24.332	3.655	100	2 1 1	24.257	3.666	100
3 1 0	31.574	2.831	45	3 1 0	31.480	2.840	60
2 2 2	34.678	2.585	63	2 2 2	34.566	2.593	80
3 2 1	37.551	2.393	28	3 2 1	37.432	2.401	42
4 0 0	40.253	2.239	5	4 0 0	40.123	2.246	27
3 3 0 4 1 1	42.808	2.111	64	3 0 0 4 1 1	42.671	2.117	78
3 3 2	47.595	1.900	5	3 3 2	47.438	1.915	19
4 2 2	49.840	1.828	15	4 2 2	49.690	1.833	22
4 3 1 5 1 0	52.028	1.756	23	4 3 1 5 1 0	51.867	1.761	45
5 2 1	56.221	1.635	4	5 2 1	56.026	1.640	22
4 4 0	58.231	1.583	20	4 4 0	58.045	1.588	39
4 3 3 5 3 0	60.200	1.536	23	4 3 3 5 3 0	60.012	1.540	38
4 4 2 6 0 0	62.136	1.493	18	4 4 2 6 0 0	61.942	1.497	30
5 3 2 6 1 1	64.036	1.453	17	5 3 2 6 1 1	63.836	1.457	35
6 2 0	65.907	1.416	4	6 2 0	65.699	1.420	10
5 4 1	67.750	1.382	11	5 4 1	67.537	1.386	18
6 2 2	69.571	1.350	15	6 2 2	69.346	1.354	29
6 3 1	71.374	1.321	8	6 3 1	71.141	1.324	26
4 4 4	73.154	1.293	9	4 4 4	72.908	1.296	22
5 4 3 5 5 0 7 1 0	74.920	1.267	4	5 4 3 5 5 0 7 1 0	74.662	1.270	17
6 4 0	76.676	1.242	5				
5 5 2 6 3 3 7 2 1	78.408	1.219	17	5 5 2 6 3 3 7 2 1	78.135	1.222	34
6 4 2	80.133	1.197	5	6 4 2	79.851	1.200	15
7 3 0	81.860	1.176	5	7 3 0	81.558	1.179	15
6 5 1 7 3 2	85.267	1.137	7	6 5 1 7 3 2	84.950	1.140	18
5 5 4 7 4 1 8 1 1	88.639	1.103	9	5 5 4 7 4 1 8 1 1	88.327	1.106	19

TABLE III

THE RESULTS OF THE HIGH-TEMPERATURE OXIDATION EXPERIMENTS

No.	Starting material	Temperature (K)	Duration (hr)	Products	Cell parameter (Å)
1	Polycrystalline	800	0.5	SOD[a] $x = 0$	8.931(1)
2	Polycrystalline	800	1.0	SOD; $x = 0.15$	8.938(2)
3	Polycrystalline	800	3.0	SOD; $x = 0.4$	8.952(2)
4	Polycrystalline	1050	0.5	SOD; $x = 1.0$	8.964(1)
5	Polycrystalline	1050	1.0	SOD; $x = 1.3$	8.975(3)
6	Polycrystalline	1050	3.0	Nepheline (decomposition)	
7	Single crystal	1050	0.5	SOD; $x = 1.0$	8.962(2)
8	Single crystal	1050	1.0	SOD; $x = 1.3$	8.973(3)
9	Single crystal	1050	3.0	SOD; $x = 1.7$	8.989(3)

[a] SOD, Sodalite $Na_8[AlSiO_4]_6(NO_2)_{2-x}(NO_3)_x$.

tures used here. With a rise in temperature, an increasing formation rate of nitrate from nitrite could be determined. The maximum NO_3^- enclosure could be observed during synthesis at 970 K.

The average dimensions of the dodecahedral-shaped crystals reached about 0.75 mm after 2 days of reaction time in the examined temperature interval. The X-ray powder data of the products with the lowest and highest nitrate content (Nos. 2 and 4, Table I) are summarized in Table II. EDAX analysis reveal an Si/Al ratio of 1.0, indicating an ordered aluminosilicate framework (calculated cell content, based on Si + Al = 12: Si 6.03; Al 5.97; Na 7.86). Due to the difficulties of microanalysis of nitrogen oxides and the low yields of the runs, making wet chemical analysis unapplicable, thermogravimetric analysis is used here to determine the nitrite–nitrate content of the crystals. Thus the products of the 970 K run led to the assumption of an imbibition of nearly 90% $NaNO_3$ beside 10% of nitrite.

High-Temperature Oxidation in Air (Indirect Preparation Method)

The results of the high-temperature oxidation experiments are summaried in Table III. At the lowest temperature (800 K) studied here, only a very small extent of the oxidation reaction could be observed at prolonged times of heating. A temperature of 1050 K was determined to be suitable for the indirect preparation of nitrate/nitrite sodalites, whereas the results obtained seem to be independent of the flow rate of air through the heating device. Somewhat different results were obtained for the reaction kinetics of the initial polycrystalline powder samples from the low-temperature synthesis compared with the single crystals from the high-temperature hydrothermal run. A maximal oxidation of about 60% of the imbibed nitrite was found for the polycrystalline powder during heating at 1050 K in an air stream of 20 liters/hr after a reaction time of 1 hr. An increase of the unit cell parameter from $a_0 = 8.931(1)$ Å to $a_0 = 8.975(3)$ Å was detected, indicating the high sensitivity of the cell volume during the incorporation of oxygen (Table III). A further oxidation of the polycrystalline samples at longer reaction times or higher temperatures (1100 K) could not be obtained, because the transition sequence sodalite–carnegeite–nepheline already starts at temperatures ≥ 1000 K due to the poor quality of the small crystallites from low-temperature synthesis. On

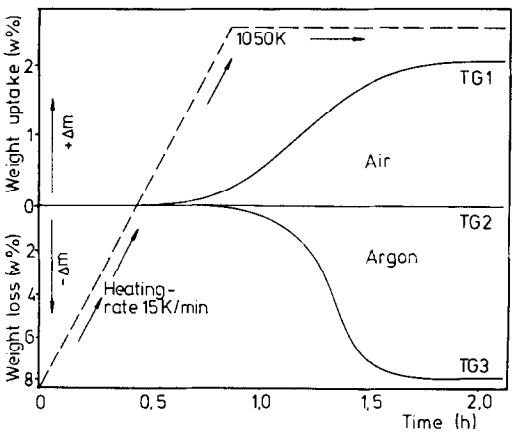

FIG. 1. Thermogravimetric plot during heating of nitrite sodalite single crystals: TG1, tempering in an air stream of 20 liters/hr leads to an increase in weight due to uptake of oxygen during the nitrate formation. TG2, heating of nitrate sodalite in air (sample No. 4, Table I). TG3, Thermal decomposition of nitrite (nitrate) sodalite (sample No. 2, Table I) during heating in an Ar atmosphere.

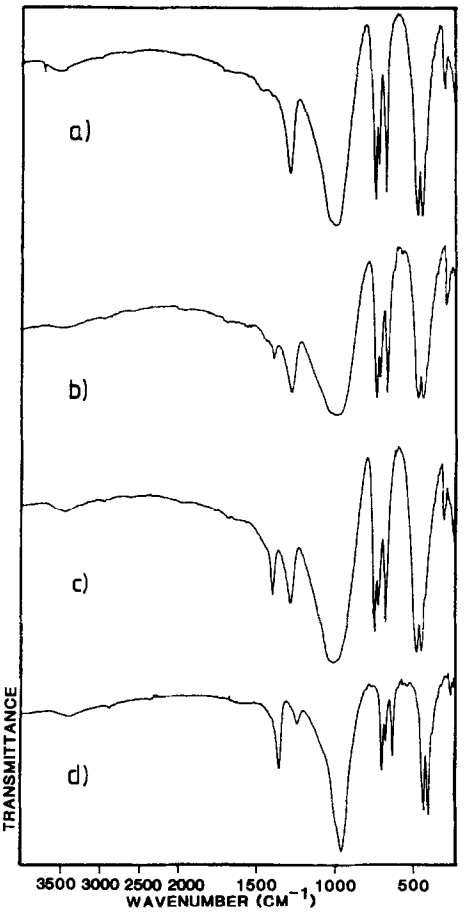

FIG. 2. IR spectra of the products from the hydrothermal syntheses (Nos. 1–4, Table I): (a) Nitrite sodalite ("reference" from low-temperature run); (b) Nitrite (nitrate) sodalite, grown at 770 K; (c) Nitrite/nitrate sodalite, grown at 870 K; (d) Nitrate (nitrite) sodalite, grown at 970 K.

the contrary, a further heating of the more stable single crystals yields sodalites, imbibing more than 90% nitrate within their cages (a_0 = 8.989(3) Å). The extent of the oxidation reaction could also be estimated by the continuous weight uptake according to TGA as demonstrated in Fig. 1 as well as from IR spectroscopic investigations described in the following section.

IR Spectroscopy

Infrared spectroscopy is suitable for the determination of the cage filling species, i.e., the guest molecules, by their specific absorption bands: NO_2^- 1270 cm^{-1}; NO_3^- 1385 cm^{-1}; OH^- 3640 cm^{-1}; and H_2O 3600–3100 cm^{-1} (*14*). The IR spectra of the synthesized sodalites are shown in Figs. 2a–2d (for direct hydrothermal synthesis) as well as in Figs. 3a–3a and 4a–4d (for the indirect preparation method). The reference spectrum (Fig. 2a) of a sample grown under low-temperature conditions as described in (*10*) indicates its pure nitrite character (with a small amount of imbibed hydrated hydroxyl groups), whereas the spectra from the species grown at 770 and 870 K clearly show a NO_2/NO_3 mixture within the sodalite cages (proportions of 4 : 1 at 770 K and 1 : 1 at 870 K). The IR spectrum of the 970 K crystals reveals the high degree of nitrate imbibition of 90%. The evolution of the nitrate band during heating of the polycrystalline samples and single crystals and the de-

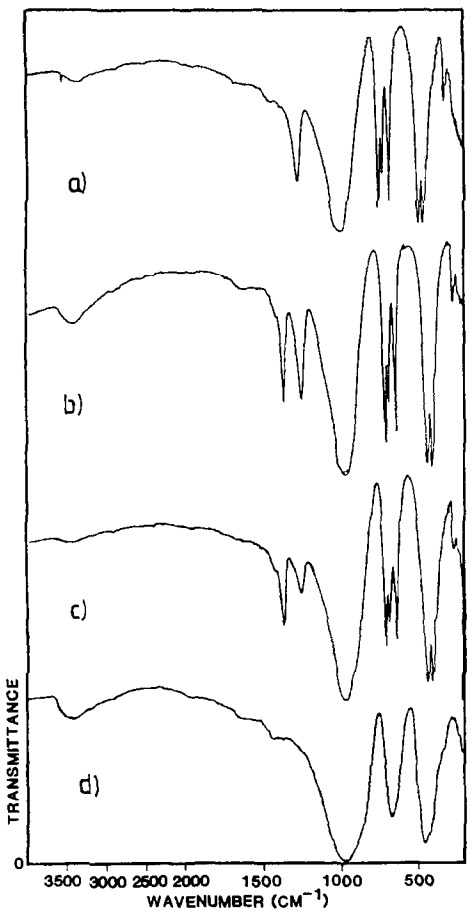

FIG. 3. IR spectra for the polycrystalline powders from isothermal heating experiments (1050 K) at different reaction times; (a) initial species; (b) 0.5 hr (No. 4, Table III); (c) 1.0 hr (No. 5, Table III); (d) 3.0 hr (No. 6, Table III).

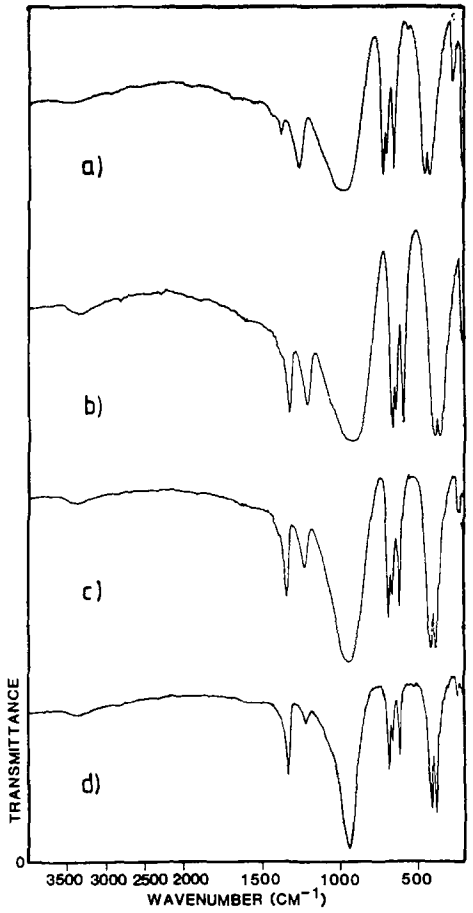

FIG. 4. IR spectra for the single crystals from isothermal heating experiments (1050 K) at different reaction times; (a) initial species; (b) 0.5 hr (No. 7, Table III); (c) 1.0 hr (No. 8, Table III); (d) 3.0 hr (No. 9, Table III).

composition of the powdered species from low-temperature synthesis (Fig. 3d) can clearly be seen from Figs. 3 and 4.

The increase of the unit cell parameter with rising nitrate content can also be confirmed by the decrease in frequency of the *T–O–T* vibration bands in the midinfrared region (750–640 cm^{-1}) (15–17).

Thermoanalytical Investigations

The samples with the lowest and highest nitrate enclosures (No. 2 and No. 4, Table I) were further studied by thermoanalytical methods. The results of the simultaneous thermal analysis in an inert atmosphere (Ar) are shown in Figs 5a and 5b. During heating of nitrite/nitrate sodalite (No. 4, Table I) a one-step decomposition reaction takes place. At elevated temperatures (1060 K according to the DTA–DTG maxima) destruction of the sodalite framework and decomposition of the imbibed NO_2 (NO_3) occurs. This process starts at 950 K and becomes very strong with a DTG/DTA maximum at

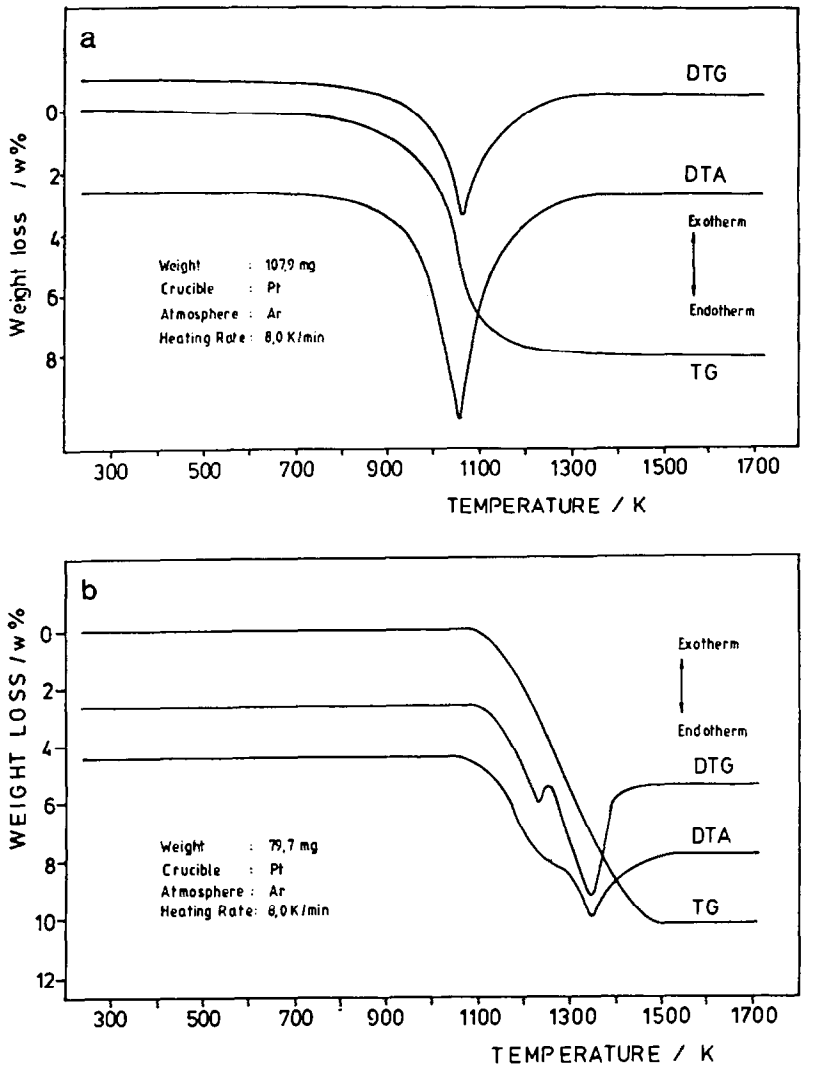

FIG. 5. Simultaneous thermal analyses of nitrite/nitrate sodalites in an innert atmosphere (Ar): (a) nitrite (nitrate) sodalite No. 2, Table I; (b) nitrate (nitrite) sodalite No. 4, Table I.

1050 K (weight loss: 8%). After total destruction of the sodalite framework at the end of this step, the Guinier–Simon photograph indicates the formation of nepheline; this is in contrast to the pure nitrite sodalite powder grown under mild conditions, where the existence of a stuffed carnegeite phase had been revealed (*10*).

The results from the high-temperature X-ray powder diffraction studies are summarized in Table IV. During the thermal decomposition process, a characteristic variation of the unit cell volume could be observed from the shift of the reflections on the Guinier–Simon photograph. The continuous rise of the cell volume is due to regular thermal expansion up to temperatures of 970 K (sample No. 2, Table I) or 920 K for the

TABLE IV

THE RESULTS FROM THE GUINIER–SIMON HIGH-TEMPERATURE X-RAY POWDER DIFFRACTION EXPERIMENTS

	Nitrite (nitrate) sodalite No. 2, Table I	Nitrate (nitrite) sodalite No. 4, Table I
Cell volume at 295 K	717.6 Å^3	726.1 Å^3
Temperature of framework expansion	970 K	920 K
$+\Delta V$ at 1050 K	7.2%	6.0%
Start of the denitrification (open conditions)	1070 K	1120 K
Decomposition product	Nepheline	Nepheline

nitrate-rich sodalite (sample No. 4). At higher temperatures an abrupt volume expansion of 7.2% (No. 2) or 6.0% (No. 4) could be observed up to the beginning of the high-temperature decomposition, i.e., with the start of the denitrification process at elevated temperatures (Table IV). The thermal decomposition behavior of nitrate (nitrite) sodalite (No. 4, Table I) differs somewhat during the decomposition step at elevated temperatures, compared with the nitrite-rich sample (No. 2, Table I). Here a two-step denitrification could be established from data of the simultaneous thermoanalysis (Fig. 5b), with DTA maxima at 1180 and 1340 K. The high-temperature total decomposition of these sodalites could not be recorded during the X-ray heating experiment because the upper limit of the heating device is 1100 K. The X-ray powder diagram of the residue from simultaneous thermoanalysis indicates the formation of a nepheline-like phase. A total weight loss of 10% accompanies this transition step, due to the thermal decomposition of the guest salt component and the resulting release of NO_x and oxygen. The evolution of the unit cell volume during this thermal decomposition of nitrate (nitrite) sodalite is similar to the behavior of the nitrite-rich species, described above.

The thermoanalytical results indicate a high degree of temperature-induced disorder and dynamic behavior of the enclosed guest nitrite and nitrate molecules. Further experiments like inelastic neutron scattering are necessary to clarify the transition from static to dynamic orientation of the guest anions. ^{23}Na MAS NMR should also be performed for checking the possible dynamical averaging of the positions of the sodium cations within the sodalite cages.

Acknowledgments

The author thanks A. Breit for her excellent technical assistance, Dr. E.-R. Krefting for the ED analysis, and Professor Dr. J. Grobe for the permission to use the IR spectrometer in his laboratory.

References

1. R. M. BARRER AND J. F. COLE, *J. Chem. Soc. A* 1416 (1970).
2. F. HUND, *Z. Anorg. Allg. Chem.* **511,** 255 (1984).
3. J. FELSCHE AND S. LUGER, *Thermochim. Acta* **113,** 35 (1987).
4. J.-CH. BUHL, G. ENGELHARDT, AND J. FELSCHE, *Z. Kristallogr.* **182,** 50 (1988).
5. J.-CH. BUHL, G. ENGELHARDT, AND J. FELSCHE, *Zeolites* **9,** 40 (1989).
6. J.-CH. BUHL, J. LÖNS, AND W. HOFFMANN, *Z. Kristallogr.* **186,** 62 (1989).
7. D. W. BRECK, Zeolites Molecular Sieves, Wiley, New York (1974)
8. J.-CH. BUHL, CH. GURRIS, AND W. HOFFMAN, "Proceedings of the 8th International Zeolite Conference, Amsterdam 1989: Zeolites For The Nineties" J. C. Jansen, L. Moscou, and M. F. M. Post, Eds.), p. 23.
9. J.-CH. BUHL, CH. GURRIS, AND W. HOFFMANN, *Ber. Dtsch. Miner. Ges.* **1,** 19 (1989).
10. J.-CH. BUHL, G. ENGELHARDT, P. SIEGER, AND J. FELSCHE, *J. Inclusion Phenom.* (1990), submitted for publication.

11. J.-CH. BUHL, J. LÖNS, AND W. HOFFMANN, *Ber. Dtsch. Miner. Ges.* **1,** 20 (1989).
12. M. T. WELLER, G. WONG, C. L. ADAMSON, S. M. DONALD, J. J. B. ROE, *J. Chem. Soc. Dalton Trans.* 593 (1990).
13. P. KEMPA, G. ENGELHARDT, J.-CH. BUHL, J. FELSCHE, G. HARVEY, AND CH. BAERLOCHER, *Zeolites* (1990), in press.
14. M. HESSE, H. MEIER, B. ZEEH, Spektroskopische Methoden in der Organischen Chemie, Thieme Vlg. Stuttgart, New York, 1984.
15. E. M. FLANIGEN, H. KHATAMI, *Adv. Chem. Ser.* 16, 201 (1971).
16. D. TAYLOR, *Mineral. Mag.* **38,** 593 (1972).
17. CH. GURRIS, Thesis, Inst. f. Miner, Univ. Münster (1989).